




Essential Oil of *Origanum vulgare* as a Green Corrosion Inhibitor for Carbon Steel in Acidic Medium

Rachid Ihamdane¹ · Malika Tiskar¹ · Brahim Outemsa² · Lamyaa Zelmat³ · Omar Dagdag⁴  · Avni Berisha⁵ · Elyor Berdimurodov⁶ · Eno E. Ebenso⁴ · Abdelaziz Chaouch¹

Received: 7 July 2022 / Accepted: 29 January 2023 / Published online: 9 March 2023
© The Author(s) 2023

Abstract

In this study, Oregano (*Origanum vulgare*) leaf essential oil was studied as an environmental-friendly anticorrosion agent for carbon steel in aggressive hydrochloric acid. The corrosion inhibition of *O. vulgare* was characterized by surface morphology, electrochemical, weight loss, theoretical and computational methods. It was found that the highest inhibition performance of *O. vulgare* was 85.64% at 2 g/l in 1 M HCl. The results of Langmuir isotherm and adsorption thermodynamics investigation demonstrated that the *O. vulgare* inhibitor adsorbed on the metal surface by the formation of rigid covalent bonds. The adsorption and inhibition centers of the selected inhibitor were studied by the computational methods, resulting in that the hydroxyl functional groups and benzoyl rings are mainly responsible for the high inhibition efficiency.

Keywords Oregano (*Origanum Vulgare*) · Green corrosion inhibitors · Carbon steels · Acidic corrosion · Adsorption

1 Introduction

Steel-based metallic materials are widely employed as transportation pipes and cooling or heating systems in the gas–oil

industries [1–3], because these materials have superior hardness, high tensile strength and low cost [4, 5]. Carbon steel is normally severely corroded during the surface treatment, storage of gas oil, heating and cooling operations, and transportation of crude oil. The reason for this is that Fe is a more reactive metal; it can easily react with the water and oxygen molecules to form the corrosion products on the metal surface. In the acid-cleaning processes of metal surfaces, the hydrochloric acid solution is normally employed to remove the oxide deposits on the surface of steel [6, 7]; as a result, a large number of corrosion products on the metal surface were depleted [8–10]. For example, the salts are accumulated inside steel-based pipes during crude oil transportation. Then, the acidic solutions are performed to clean the metal surface [2, 11]. However, the corrosive nature of these acids leads the metal to dissolve during cleaning procedures, resulting in the deterioration of the metal substrate [12, 13]. The addition of a corrosion inhibitor to the corrosive medium is a cost-effective way for the metal protection from acidic attack. Corrosion inhibitors are water-soluble compounds, and they are added to the pickling solution at low concentrations [2]. At that point, the metal surface is effectively insulated from the corrosion attacks of acidic solution [14–16]. Traditional inhibitors have harmful environmental effects. Due to their harmful impact on individuals and the environment, the use

-
- ✉ Omar Dagdag
dagdao@unisa.ac.za
- ✉ Elyor Berdimurodov
elyor170690@gmail.com
- ✉ Eno E. Ebenso
ebensee@unisa.ac.za

- ¹ Laboratory of Organic Chemistry, Catalysis and Environment, Department of Chemistry, Faculty of Sciences, Ibn Tofail University, BP 133, 14000 Kenitra, Morocco
- ² Laboratory of Agro-physiology, Biotechnology, Environment and Quality, Department of Biology, Ibn Tofail University, BP 133, 14000 Kenitra, Morocco
- ³ Plant, Animal Productions and Agro-Industry Laboratory, Faculty of Sciences, Ibn Tofail University, Kénitra, Morocco
- ⁴ Centre for Materials Science, College of Science, Engineering and Technology, University of South Africa, Johannesburg 1710, South Africa
- ⁵ Department of Chemistry, Faculty of Natural and Mathematics Science, University of Prishtina, 10000 Prishtina, Kosovo
- ⁶ Faculty of Chemistry, National University of Uzbekistan, 100034 Tashkent, Uzbekistan



of these inhibitors has been limited [17, 18]. This has augmented ecological awareness, and the use of green corrosion inhibitors has gained greater consideration recently [19–24].

Green inhibitors are natural [25–27], non-toxic, environmentally friendly [28, 29], readily available and renewable products to prevent metal from corrosion, such as plant extracts and essential oils, which have more functional groups (carboxyl, hydroxyl and amino), aromatic rings and hetero atoms. These features promote their high corrosion efficiency [30–33].

Origanum vulgare (Oregano) is a native herb of the middle countries and belongs to the family Lamiaceae. The essential oil of *O. vulgare* contained more phenol compounds, such as hydroxycinnamic acid, caffeic acid, rosmarinic acid and other acid compounds [34], indicating that these biologically active compounds are good adsorbents on the metal surface.

The main aim of this investigation is to explore the inhibition efficiency of the essential oil of *O. vulgare* for steel in 1 M HCl medium as an environmental-friendly agent for mild steel by the surface morphology, electrochemical, weight loss, theoretical and computational methods.

2 Experimental

2.1 Materials and Methods

2.1.1 Preparation of Inhibitor and Corrosive Environment

In this investigation, carbon steel was used as the working electrode. Its chemical composition is listed in Table 1. The working electrodes, whose contact surface with the corrosive medium is 1 cm², were prepared by polishing them with 80-to-2000-grit emery paper, then washing and drying them with distilled water and acetone. A 1 M solution of hydrochloric acid was used to prepare the corrosive solution. The corrosive hydrochloric acid solutions were made by diluting 37% HCl with deionized water.

2.1.2 Preparation of Inhibitor

The essential oil Oregano was used as the selected inhibitor. Oregano samples were collected from the region of *Lekhmisset* (Morocco). The dried aerial components were hydro-distilled for 4 h by a Clevenger-type device. The essential oil was extracted, dried with anhydrous sodium sulfate and kept at 4 °C until it was needed. The essential oil of Oregano extracted by Ghanmi et al. [35], in which the major compounds are presented in Fig. 1 and Table 2, was used in a concentration range from 0.5 to 2 g/l.

2.2 Weight Loss Study

The dimensions of the utilized steel samples are 1.5 cm × 1.5 cm × 0.05 cm. The weight loss of metal coupons was measured after corrosion and inhibition according to ASTM G1-67 standard after 6 h of immersion time. The protection performance (E_W , %) and corrosion rate (W_{corr}) are estimated by Eqs. (1) and (2), respectively, in which W_{corr} is the corrosion rate in the corrosion solution, $W_{\text{corr/inh}}$ is the corrosion rate in inhibited solution, Δm is weight loss in mg, t is immersion time in hours and S is surface area in cm²,

$$E_W\% = \frac{W_{\text{corr}} - W_{\text{corr/inh}}}{W_{\text{corr}}} \times 100 \quad (1)$$

$$W_{\text{corr}} = \frac{\Delta m}{S \times t} \quad (2)$$

2.3 Electrochemical Study

Using a PGZ100 galvanostat potentiostat equipped with Volta Master 4 software and a three-electrode cell containing a working electrode (plain steel), a saturated calomel reference electrode (ECS) and a chemically inert counter electrode (platinum), the electrochemical tests were conducted. The system was connected to a computer. To get the OCP constant, the working electrodes were submerged in the solution for 0.5 h.

The electrochemical potential reached a steady state during 0.5 h. The PDP analysis was done between – 900 and – 100 mV. The values of protection degrees were calculated using Eq. (3), where i_{corr}^0 and i_{corr}^i show the corrosion current densities for corroded and inhibited metal samples, respectively.

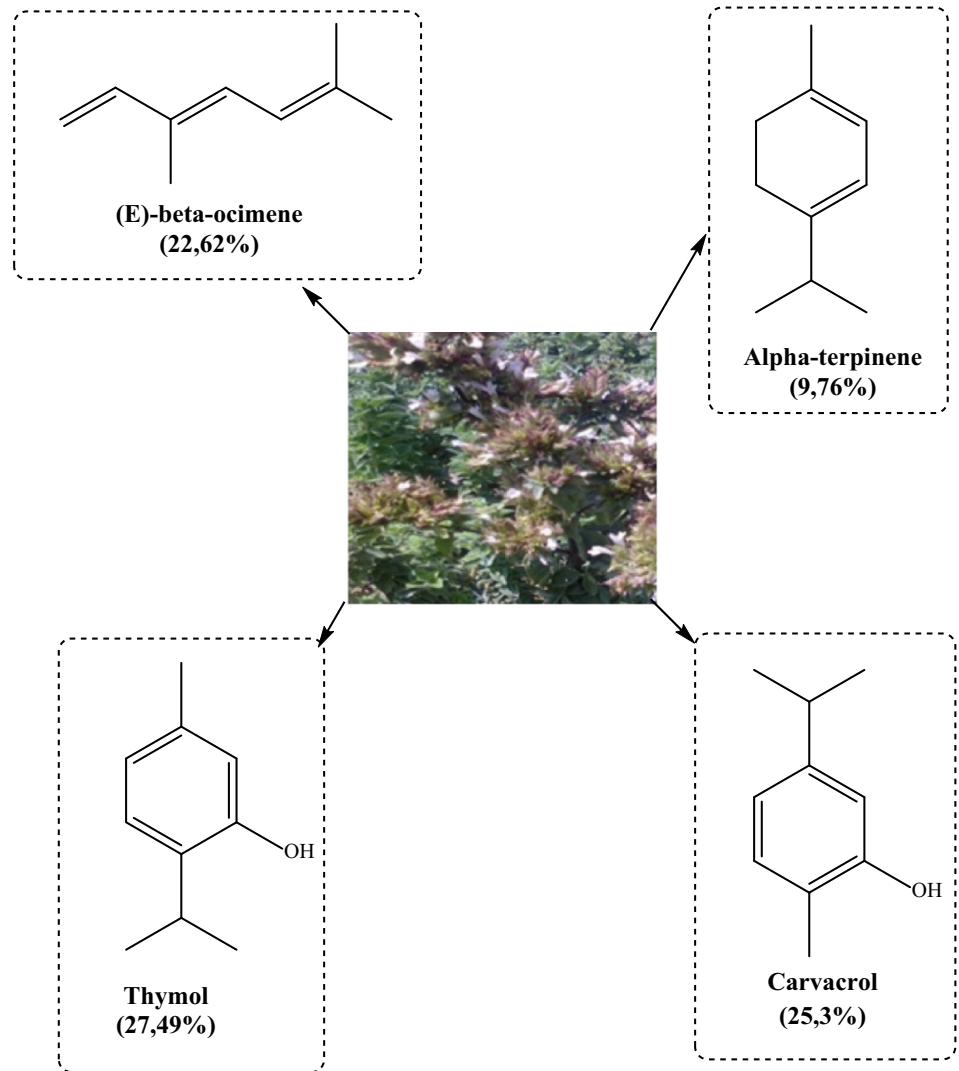
$$\eta_{\text{PDP}}(\%) = \frac{i_{\text{corr}}^0 - i_{\text{corr}}^i}{i_{\text{corr}}^0} \times 100 \quad (3)$$

The next part of electrochemical measurement is EIS, which was done between 100 kHz and 100 mHz with the 10 mV applied AC signal. It is noted that a thermostat bath was used to keep the solution temperature at the targeted value. The protection degrees of selected inhibitors were estimated using Eq. 4, where R_{ct}^i and R_{corr}^o are the charge transfer resistances in the inhibitor-free and inhibitor-contained systems.

$$\eta_{\text{EIS}}(\%) = \frac{R_{\text{ct}}^i - R_{\text{corr}}^o}{R_{\text{ct}}^i} \times 100 \quad (4)$$

Table 1 Chemical composition of selected carbon steel

Element	V	Co	Cu	Al	Ni	Mo	Cr	Mn	Si	C	W	Fe
wt%	< 0,003	< 0,0012	0,14	0,03	0,1	0,02	0,01	0,47	0,24	0,11	0,06	rest

Fig. 1 Major phytochemicals present in the plant Oregano (*Origanum vulgare*)**Table 2** Basic compounds of the essential oil of Oregano

IK	Component	(%)
1016	α -terpinene	9,76
1046	(E)-beta-ocimene	22,62
1185	Thymol	27,49
1191	Carvacrol	25,3

2.4 Surface Study

The changes in the surface morphology of metal after corroding and inhibition (2 g/l inhibitors) processes were explored by scanning electron microscopy (SEM) (JOEL JSM-5500) at 20 keV (magnification is 500 \times) and 298 K. The surface destructions and improvements on the surface were identified by the SEM analysis.

2.5 Computational Investigations

2.5.1 DFT Study

The density functional theory (DFT) is frequently used in corrosion inhibition studies.

The DFT method accurately describes the performance of organic compounds as corrosion inhibitors. In this study, the DFT calculations were performed using the Biovia Materials studio program with the Dmol3 module (Biovia, USA) [36, 37]. In the geometry optimizations of selected inhibitors, the double numerical basis set with polarization (DNP) [38] and the SCAN (Strongly Constrained and Appropriately Normed) functional [39, 40] in the frame of Generalized Gradient Approximation [41] were used. The DFT calculations were performed in the solvent (water) via a Conductor-like Screening Model (COSMO) [42, 43].

2.5.2 MC and MD Simulations

The chemical interactions between the metal surface and selected corrosion inhibitors were theoretically investigated by the monte carlo (MC) and molecular dynamic (MD) simulations. The simulation analyses were performed in Material Studio (Biovia, USA) using COMPASS III (Version 1.0) force-field (condensed phase), Forcite module and NVT canonical ensemble at 298 K (simulation time is 1 ns) [6, 44, 45]. Before undertaking simulations, the whole system was geometrically optimized [46–48]. The temperature of the simulation box was controlled by the Berendsen thermostat [49–51]. The radial distribution function (RDF) was also studied in this analysis [52]. The adsorption sites, energies and chemical adsorption mechanisms were also predicted in this analysis. These simulations were done on Fe(110) iso-surface (three dimensions to the slab model: 14.260 Å × 19.8590 Å × 19.8590 Å) under periodic boundary conditions. This model included 10 hydronium, 10 chloride, 350 H₂O molecules and 1 inhibitor molecule.

3 Results and Discussion

3.1 Weight Loss Study

The first way to evaluate the corrosion inhibition of a metal in an electrolyte solution is through weight loss method. The advantage of this approach is that it does not require a lot of equipment. The results of the weight loss tests are indicated in Table 3. It is noted that the inhibition efficiency and corrosion rate depend on the change in the concentration, confirming that the maximal protection degree was 85.64% while the minimal corrosion rate was 0.115 mg/cm²*h at 2 g/l. This demonstrates that the chosen essential oil is an

Table 3 Weight loss analysis results of steel in the absence and presence of Oregano extract at different concentrations and 308 K in 1 M HCl

	C (g/l)	W_{corr} (mg/cm ² *h)	E_W (%)
1 M HCl	0	0,801	–
Oregano extract	0.5	0,215	73,16
	1	0,21	73,78
	1,5	0,195	75,65
	2	0,115	85,64

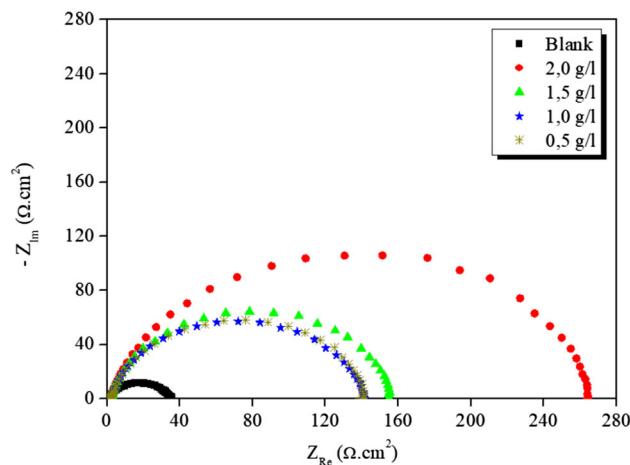


Fig. 2 Nyquist diagrams for blank and corrosion inhibitors of the essential oil of oregano at various concentrations

effective inhibitor for steel corrosion in 1 M HCl. This is due to this extract having good organic compounds, in which the aromatic rings are the main sign of the high inhibition. The aromatic rings are abundant in delocalized π -electron systems. This accounts for the excellent inhibition performance. With the support of π -electron systems, the inhibitor adsorbed onto the metal surface by forming strong covalent bonds.

3.2 Electrochemical Studies

3.2.1 EIS

EIS is regarded as one of the most prevalent and effective techniques; its purpose is to identify various electrochemical reaction phenomena and protective mechanisms [53]. Figure 2 represents the electrochemical impedance diagrams for blank and inhibitor in 1 M HCl. It is noted from these results that the presence of a single capacitive half-loop indicates that the corrosion and inhibition of metal surface are mainly controlled by the process of charge transfer [54], and the increase in the concentration of inhibitor is attributed to the rise the diameter of the capacitive loop. This effect

Table 4 Electrochemical parameters of the impedance diagram of steel in 1 M HCl in the presence of the essential oil of Oregano extract at different concentrations at 298 K

	C (g/l)	R_s ($\Omega\cdot\text{cm}^2$)	R_{ct} ($\Omega\cdot\text{cm}^2$)	C_{dl} ($\mu\text{F}\cdot\text{cm}^{-2}$)	n_{dl}	Q ($\mu\text{F}\cdot\text{S}^{n-1}$)	η_{EIS} (%)
1 M HCl	–	1.12	34.7	121.0	0.773	419	–
Oregano extract	2.0	1.84	263.3	48.4	0.877	83	86.8
	1.5	2.21	153.6	82.9	0.890	133	77.4
	1.0	2.35	140.0	83.5	0.887	137	75.2
	0.5	2.52	138.2	90.3	0.895	142	74.9

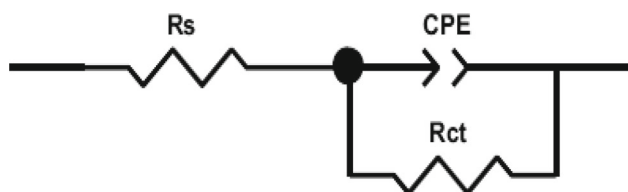


Fig. 3 An equivalent circuit model (EIS)

is responsible for enhancing the protective power of the inhibitor [55, 56].

Table 4 summarizes the electrochemical parameters obtained by modeling the impedance spectra using the following equivalent circuit (Fig. 3). According to Table 4, when the inhibition concentration rises, then the double-layer capacitance C_{dl} was decreased up to a value of $48.4 \mu\text{F}/\text{cm}^2$, while the charge transfer resistance was increased significantly reaching a maximum of $263.3 \Omega\cdot\text{cm}^2$ at 2 g/l. According to the literature [14], these observations can be interpreted and confirmed. These results also suggested a higher inhibition ability of the selected inhibitor. Oregano extract contained more hydroxyl functional groups, which are attached to benzoyl rings. These functional groups are effectively adsorbed to the metal surface by the formation of covalent bonds. Consequently, a protective film was formed on the steel surface. According to Qian et al. and Mourya et al. [57, 58], the corrosion inhibitor electrostatically and chemically adsorbs on the metal surface, displacing the water molecules adsorbing on the surface. As a result, the values in double-layer capacitance (C_{dl}) markedly went down. The next reason for this decrease is that the defender layer was formed on the metal surface by the adsorption of corrosion inhibitors. The C_{dl} is characterized related to Eq. (5), in which S is the metal surface dimension, d is the dielectric constant, ϵ is the environment constant and ϵ_0 is vacuum constant [59].

$$C_{dl} = \frac{\epsilon\epsilon_0}{d} S \tag{5}$$

The protection values given in Table 4 show that the essential oil of oregano admits a good inhibitory power with a maximum inhibitory efficiency of 86.8% at 2 g/l. The values in charge transfer resistance (R_{ct}) and solution resistance

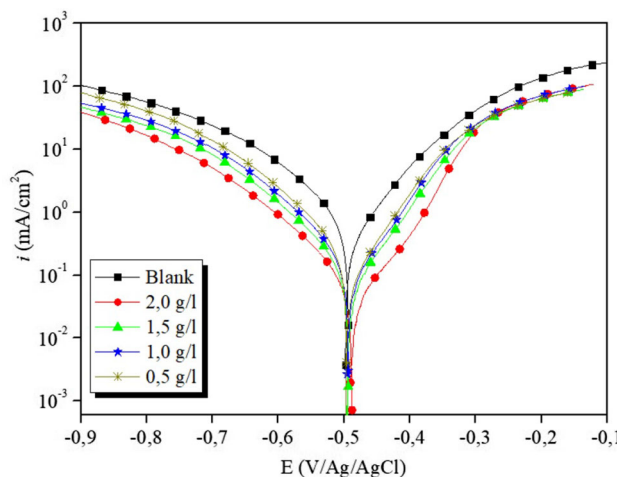


Fig. 4 Polarization curve of steel in 1.0 M HCl (Blank and essential oil of oregano extract at different concentrations)

(R_s) are high in the corrosion solution, because the metal surface was corroded. In comparison, the values of R_s and R_{ct} decrease with the presence of corrosion inhibitors. This is due to the formation of a protective film.

3.2.2 PDP

The electrochemical kinetic character of the metal/electrolyte interface was identified by PDP methods. Figure 4 indicates the Tafel curves obtained in the presence and absence of the essential oil of Oregano in a 1 M HCl medium. It is also demonstrated that the presence of *oregano* essential oil has a small effect on the anodic curves, whereas the addition of corrosion inhibitors reduces the corrosion density relative to the control. This suggests that the development of a protective coating reduces the rate of anodic and cathodic corrosion. Corrosion inhibitors have an effect on anodic corrosion (iron oxidation) and cathodic hydrogen reduction [60]. The values of EIS functions were found by extrapolation of the Tafel plots; the obtained data are indicated in Table 5. It is clear from the obtained results that (1) the selected corrosion inhibitor is a mixed type, which means that the corrosion and inhibition processes were depleted by the cathodic and anodic interactions; (2) the potential differences among the

Table 5 Electrochemical parameters of the essential oil of Oregano extract at different concentrations at 298 K

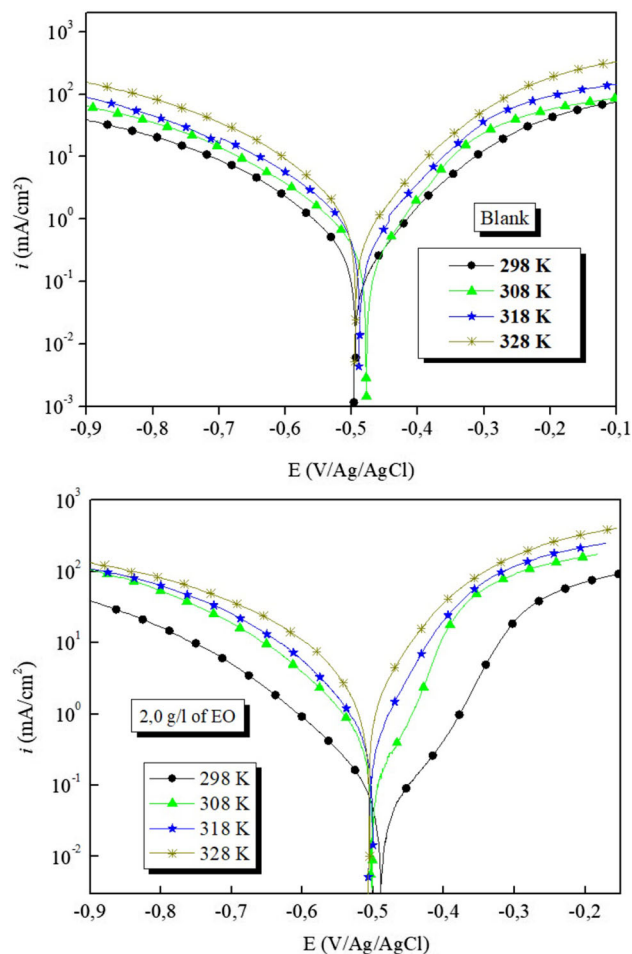
	C (g/l)	$-E_{\text{corr}}$ (mV/Ag/AgCl)	i_{corr} ($\mu\text{A}/\text{cm}^2$)	$-\beta_c$ (mV/dec)	β_a (mV/dec)	η_{PDP} (%)
1 M HCl	–	498	983	140	150	–
Oregano extract	2.0	486	122	126	135	87.5
	1.5	492	213	124	137	78.4
	1.0	491	236	126	140	75.9
	0.5	494	242	127	146	75.3

corrosion and inhibition processes were lower 80 mV, indicating that the electron transfers on the metal surface were maximally blocked with the presence of corrosion inhibitor [61]; (3) the addition of inhibitor is attributed to a decrease in the current density compared to the blank, indicating a slowdown in the rate of corrosion due to the adsorption of these molecules on the metal surface [62]. The obtained EIS data show that the selected compound protects 87% of the metal surface from corrosion attacks at 2 g/l.

Temperature Effect The temperature is also the next important effect on corrosion and inhibition. The rise of the temperature modifies the inhibition and adsorption characteristics. The corrosion reactions are rose, and the adsorption processes are reduced with the rise of temperature. The literature indicates that the inhibitory actions of essential oils are temperature dependent [63, 64]. In the present investigation, the temperature effect was studied by the PDP method. The results of the PDP curves at various temperatures are found in Fig. 5. According to Fig. 5, it is noted that the rise in temperature is responsible for a rise in the current density and the corrosion rate in both cases. It is also shown that the anodic and cathodic plots were decreased in the inhibited system, confirming that the selected inhibitor can protect the metal surface at high temperatures [43].

Table 6 indicates the electrochemical parameters obtained from the potentiodynamic polarization curves. It is observed that when the temperature rose, then the current density increased in both cases. The temperature rise cannot dramatically change the inhibition performances. The inhibition protection was 87.5% at 298 K while this value was 81.6% at 328 K, showing that there is little decrease in the inhibition efficiency. It is also indicated that the cathodic and anodic slopes have not been varied significantly; these observations reveal that the temperature of the medium does not affect the mechanism of protection and it acts only on the speed of the reactions involved. It decreased the speed of adsorption of essential oil of Oregano on the metal surface [65].

Changes in Activation Parameters According to the literature [66, 67], it was confirmed that the changes in activation were explored using the thermodynamic parameters such as

**Fig. 5** Potentiodynamic polarization curves of steel (2.0 g/l of essential oil of Oregano)

activation entropy, enthalpy and energy. These thermodynamic parameters can quantify the effectiveness of corrosion inhibition and identify the adsorption type. Additionally, the surface phenomenon, the interaction between the inhibitor and surface, heat treatments of inhibition and electrostatic interactions on the surface were described by the thermodynamic analysis. The dependence of the value of corrosion density (i_{corr}) to the variation in temperature can be considered related to Arrhenius Eq. (6) [68], in which the T

Table 6 Electrochemical parameters of PDP curves for steel (Essential oil of Oregano at different temperatures)

	T (K)	$-E_{\text{corr}}$ (mV/Ag/AgCl)	i_{corr} ($\mu\text{A}\cdot\text{cm}^{-2}$)	$-\beta_c$ (mV dec $^{-1}$)	β_a (mV dec $^{-1}$)	η_{PDP} (%)
Blank	298	498	983	140	150	–
	308	477	1200	184	112	–
	318	487	1450	171	124	–
	328	493	2200	161	118	–
Oregano extract	298	486	122	126	135	87.5
	308	499	168	139	101	86.0
	318	497	235	144	109	83.8
	328	503	405	180	123	81.6

Table 7 Values in thermodynamic parameters for carbon steel in 1 M HCl solutions with and without inhibitor

	E_a (kJ/mol)	ΔH_a (kJ/mol)	ΔS_a (J/mol K)
Blank	21.0	18.5	– 126.0
Oregano extract	31.8	29.2	– 107.3

is temperature, E_a is activation energy and A is constant. The thermodynamic parameters are estimated using Eq. (7), in which the ΔS_a is activation entropy, ΔH_a is activation enthalpy, h is plank constant, N is Avogadro number and R is universal gas constant.

$$i_{\text{corr}} = A \cdot \exp\left(\frac{-E_a}{RT}\right) \quad (6)$$

$$i_{\text{corr}} = \frac{RT}{Nh} \exp\left(\frac{\Delta S_a}{R}\right) \exp\left(\frac{-\Delta H_a}{RT}\right) \quad (7)$$

According to Ivanov [69], the adsorption performance of corrosion inhibitors also depends on the values of activation energy. This is due to the corrosion inhibitor adsorbed on the metal surface by the covalent and electrostatic interactions. The rise in temperature is depleted the force of electrostatic interactions [70]. Table 7 indicates that the values of activation energy were enhanced with the presence of the organic compound, confirming that the energetic blocks were formed for the corrosion processes by the formation of a protective film on the metal surface [70]. The positive value of ΔH_a indicates that the dissolution process of steel is endothermic [71]. The increase in entropy in the inhibited system confirmed that the Fe reacted with organic compounds to form the active complex, which adsorbed on the metal surface effectively [66].

3.3 Surface Morphology Analysis

The surface morphology analysis indicates the surface phenomenon and changes on the metal surface after the corrosion and inhibition processes. In this research work, the SEM observations are made on steel samples after 6 h of immersion (Fig. 6). It is revealed from Fig. 6a that the surface of the metal was seriously scratched in the acidic solution. It also noticed that the surface is importantly destroyed with the corrosion ions on the entire surface in the absence of the inhibitor system. The presence of the essential oil of Oregano in 1 M HCl solution (Fig. 6b) made the surface more smooth, confirming that the metal surface was well insulated from the acidic medium.

3.4 Theoretical Analysis

3.4.1 DFT Results

Figure 7 shows the results of the conformer search (6000 conformers found) and the corresponding lowest energy structures for α -terpinene, (E)- β -ocimene, thymol and carvacrol molecules [72–75]. As can be observed that the found lowest energy structures of α -terpinene, (E)- β -ocimene, thymol and carvacrol are efficient corrosion inhibitors.

Figure 8 shows the σ -profile of the α -terpinene, (E)- β -ocimene, thymol and carvacrol molecules. The selected inhibitors have good H-bonding acceptor and donor sites, which are responsible for the physical and chemical adsorption mechanisms. The accepting and donating abilities of the α -terpinene, (E)- β -ocimene, thymol and carvacrol molecules depend on the interaction between their functional groups and water molecules.

Figure 9 shows the optimized structures of studied molecules and the estimation of the MAC values for O atoms. As indicated, the α -terpinene, (E)- β -ocimene, thymol and carvacrol molecules were good polar organic compounds. Their high polarity is rose in the aquatic solution. The

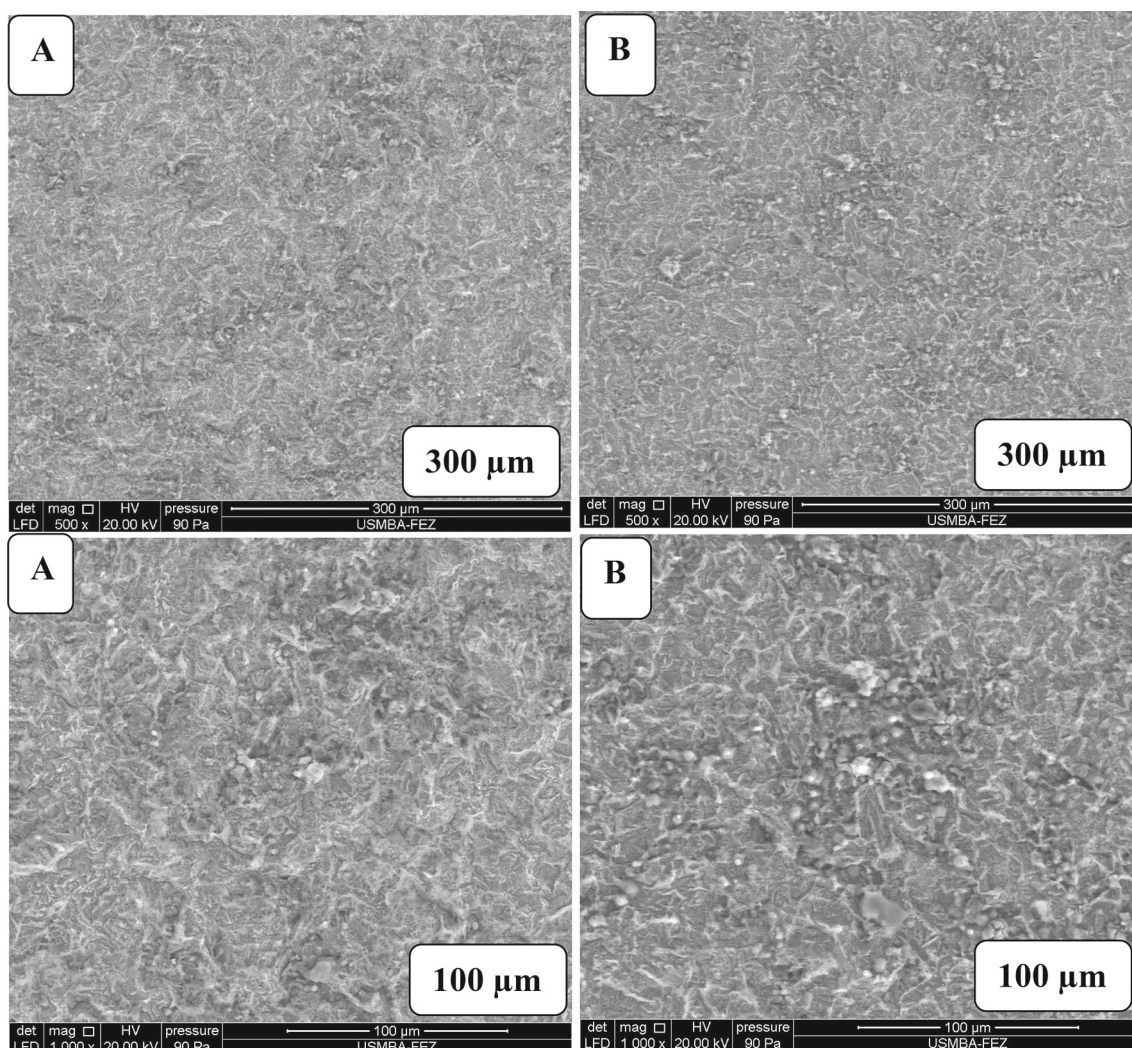


Fig. 6 SEM pictures of carbon steel surface: **a** in corrosion and **b** in inhibited systems (2 g/l, 298 K)

functional groups and delocalized aromatic systems are the main reason for their high polarity.

The Mulliken Atomic Charges (MAC) provide a consistent and convincing indicator of the inhibition adsorption heteroatoms. It is revealed that the oxygen atoms mainly interacted with the Fe atoms [72, 76–78]. Figure 10 reveals optimized structure, HOMO, LUMO and ESP pictures of α -terpinene, (E)- β -ocimene, thymol and carvacrol molecules. The values of basic theoretical parameters were found and are indicated in Table 8. Molecular activity is key to describing the chemical properties and structural positions for chemical reactions [3, 5, 7, 47]. The HOMO regions are more electron-rich. The electrons of HOMO regions are shared with electrophilic regions of the substrate. In comparison, the electrons are accepted in LUMO regions from the nucleophilic species [5]. The α -terpinene, (E)- β -ocimene, thymol and carvacrol molecules are chemically adsorbed on the

metal surface by the HOMO regions while the LUMO regions are attributed to promoting the adsorption.

Calculated theoretical parameters of α -terpinene, (E)- β -ocimene, thymol and carvacrol molecules are tabulated in Table 8 related to the previously reported equations [3, 79]. The difference between the HOMO and LUMO energy was around 4–5 eV for the studied chemicals, suggesting that they are good adsorbents on the metal surface. The values of electron affinity and ionization potential for these inhibitors were around 1 and 6 eV, respectively, confirming that the electron transfer between the vacant D-orbitals of iron and HOMO regions is very effective [3, 79]. It is also revealed that the α -terpinene, (E)- β -ocimene, thymol and carvacrol molecules are low hardness and high softness compounds, showing good corrosion efficiency. The values of energy of back-donation and fraction of transferred electrons also confirmed that the electrons of corrosion inhibitors are easily

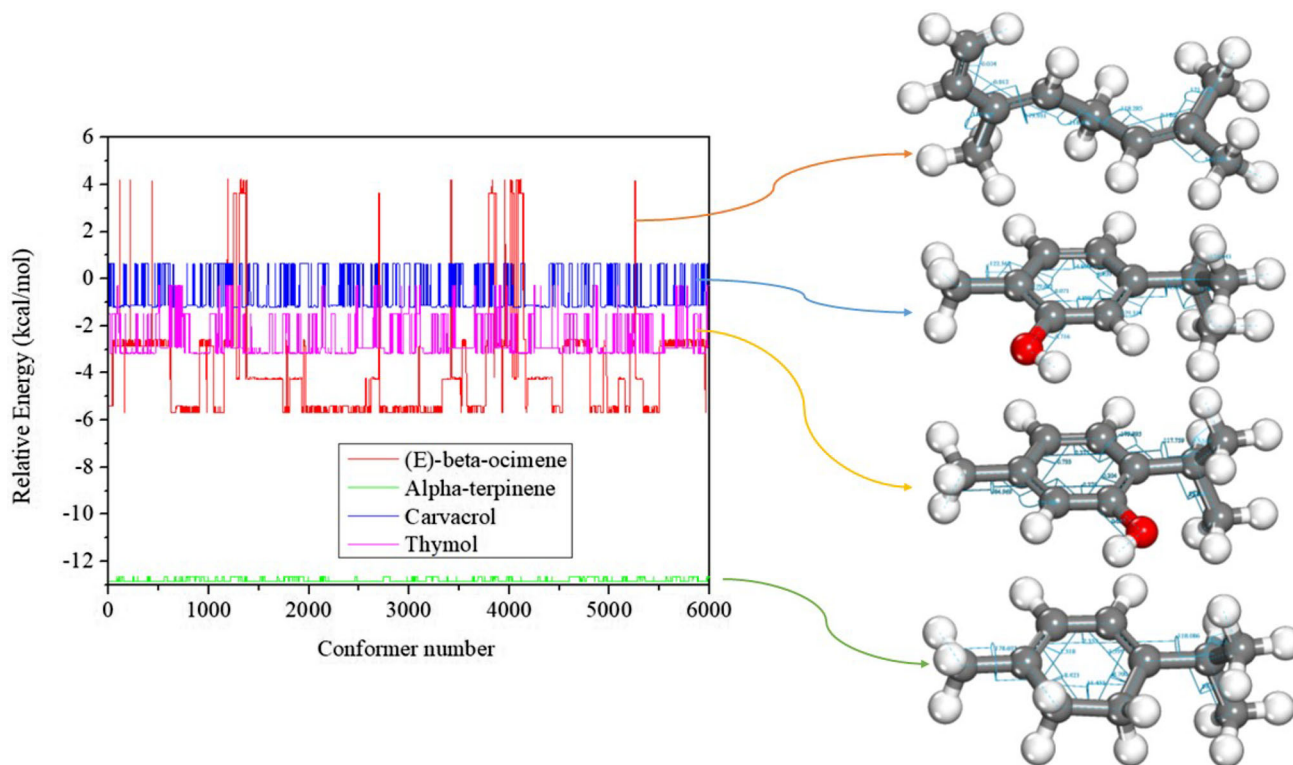
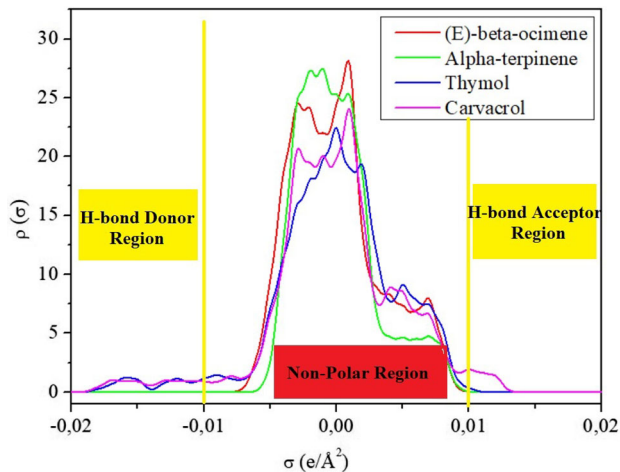


Fig. 7 Conformer search and the corresponding lowest energy structures for α -terpinene, (E)- β -ocimene, thymol and carvacrol molecules

Fig. 8 σ -profile of the α -terpinene, (E)- β -ocimene, thymol and carvacrol molecules



shared to the metal surface. As a result, the rigid donor–acceptor bonds are formed between the D-orbitals of Fe and heteroatoms of the inhibitor [80, 81].

3.4.2 MC Simulation

The interaction of the α -terpinene, (E)- β -ocimene, thymol and carvacrol molecules with the surface of Fe(110) was investigated by the MC simulations, and the obtained results

are indicated in Fig. 11. The adsorption energy (E_{ads}) may be deduced from Eq. (8), in which the $E_{inhibitor}$ is inhibition energy; $Fe(110)$ is Fe surface energy; $E_{(110)//inhibitor}$ is the total energy of the simulated system; the obtained values of E_{ads} show the adsorption forces of optimized structure [82–84].

$$E_{ads} = E_{(110)//inhibitor} - (Fe(110) + E_{inhibitor}) \quad (8)$$

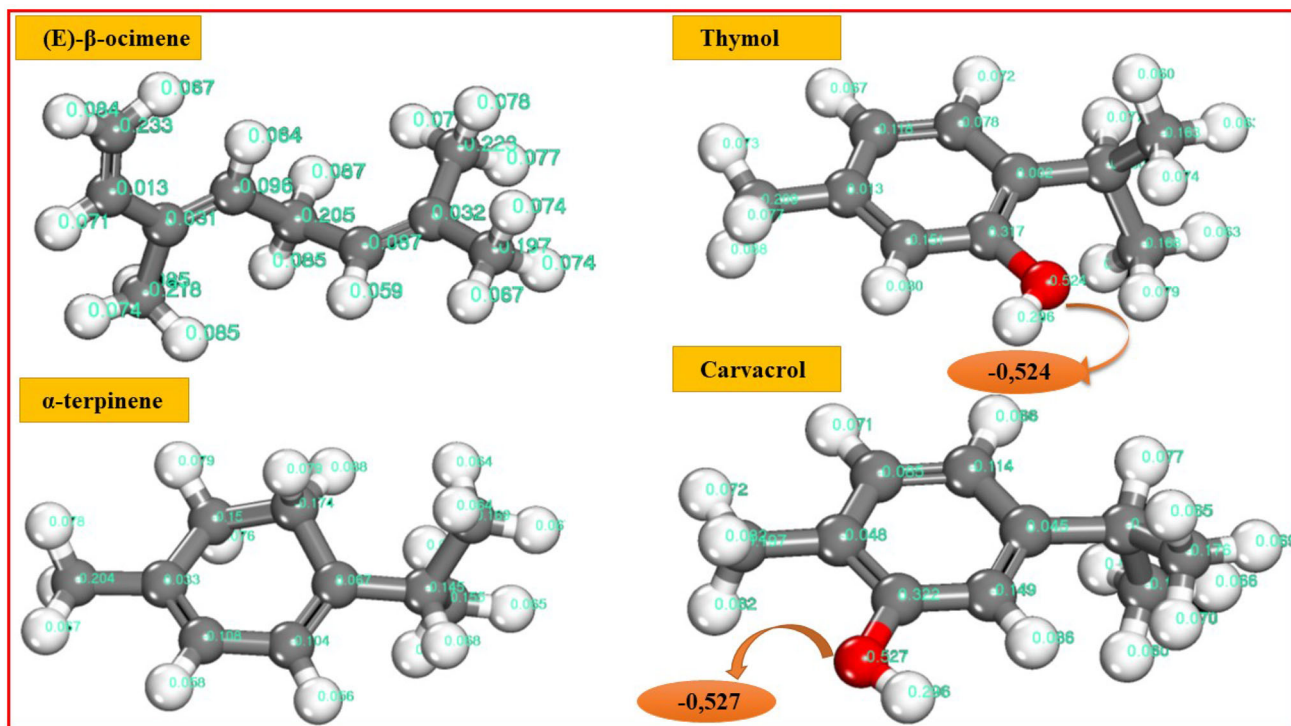


Fig. 9 Optimized structures of studied molecules and estimation of the MAC values for O atoms

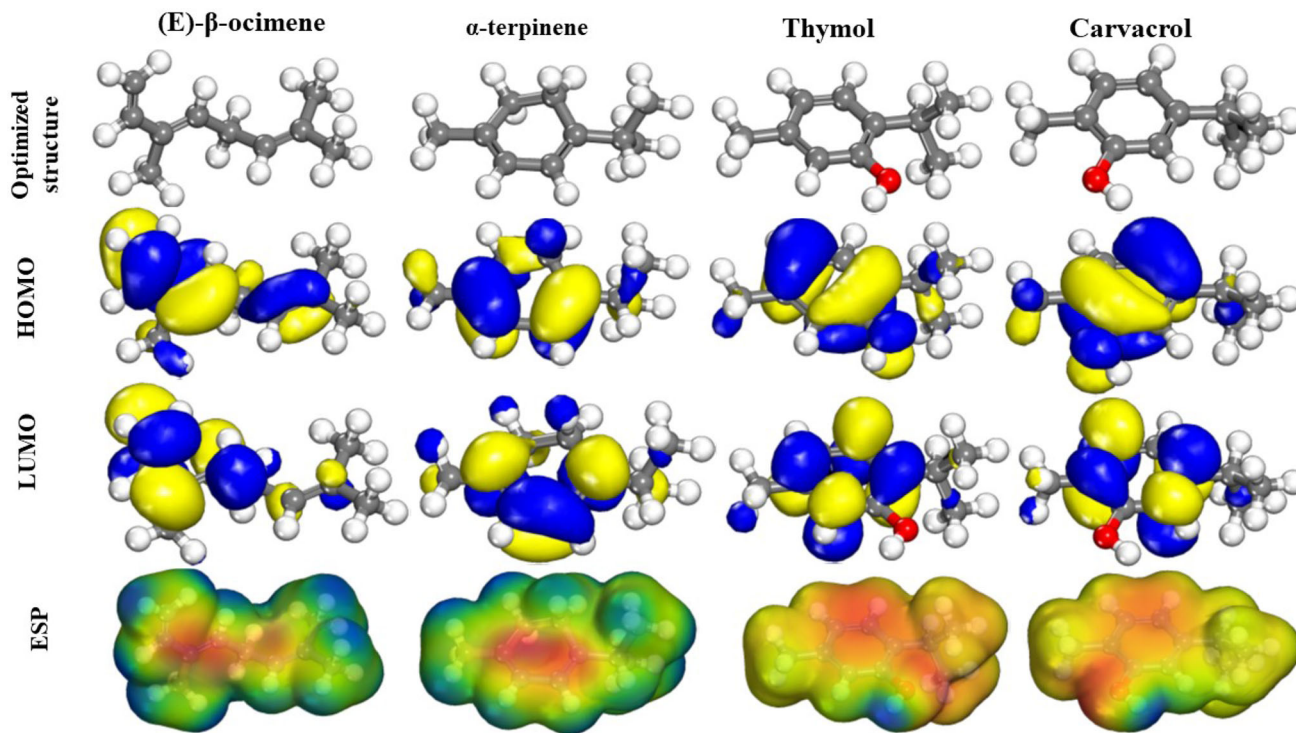


Fig. 10 Optimized structure, HOMO, LUMO and ESP pictures of α-terpinene, (E)-β-ocimene, thymol and carvacrol molecules

Table 8 Calculated theoretical parameters of α -terpinene, (E)- β -ocimene, thymol and carvacrol molecules

Theoretical parameters	α -terpinene	(E)- β -ocimene	Thymol	Carvacrol
E_{HOMO} (eV)	− 5.375	− 5.823	− 6.018	− 6.006
E_{LUMO} (eV)	− 0.488	− 0.951	− 0.156	− 0.104
$\Delta E(E_{HOMO}-E_{LUMO})$ (eV)	4.887	4.872	5.862	5.902
Ionization energy (I)	5.375	5.823	6.018	6.006
Electron affinity (A)	0.488	0.951	0.156	0.104
Electronegativity (χ)	2.931	3.387	3.091	3.055
Global hardness (η)	2.433	2.436	2.931	2.951
Global softness (σ)	0.411	0.410	0.341	0.338
Chemical potential (μ)	− 2.931	− 3.387	− 3.091	− 3.055
Fraction of transferred electrons (ΔN)	0.623	0.741	0.666	0.668
$\Delta E_{back-donation}$	− 0.608	− 0.609	− 0.732	− 0.737

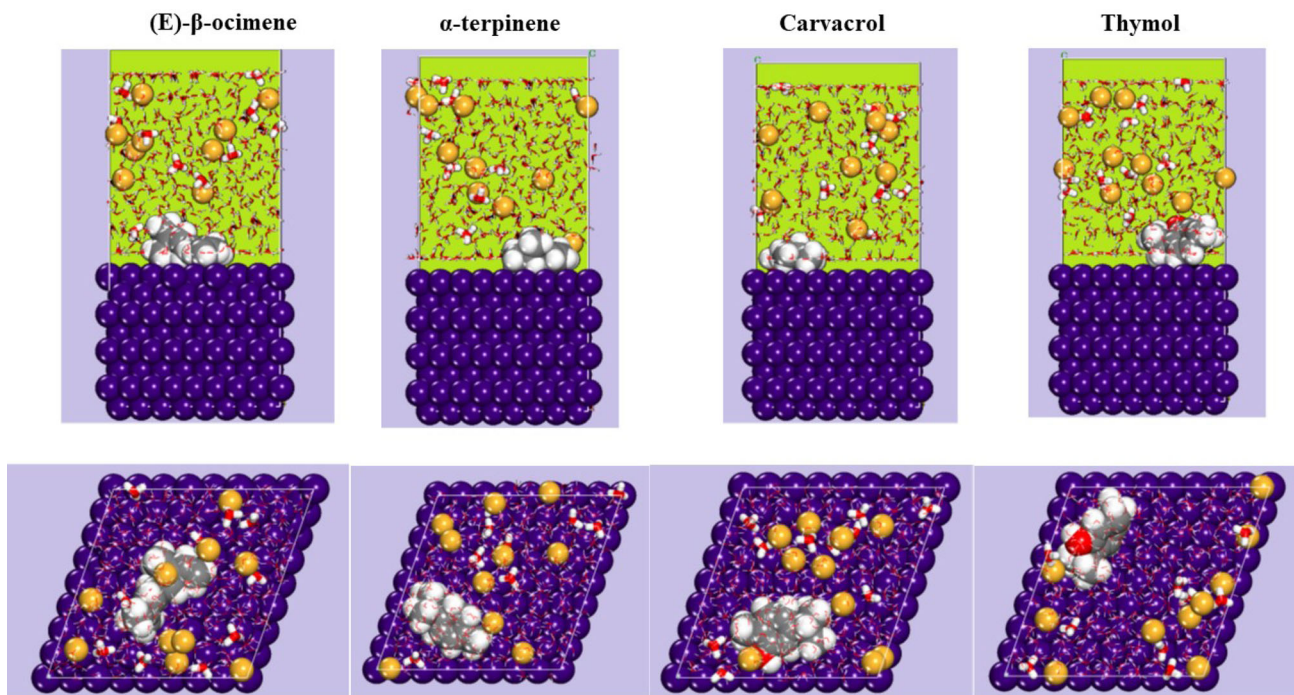


Fig. 11 MC simulations results: adsorption configurations and positions of α -terpinene, (E)- β -ocimene, thymol and carvacrol molecules on the Fe(110) surface

The adsorption configurations and positions of α -terpinene, (E)- β -ocimene, thymol and carvacrol inhibitors on the studied surface were found. Figure 12 indicates the values of adsorption for selected optimized structures show the following order of inhibition efficiency: Carvacrol > (E)- β -ocimene > α -terpinene = Thymol (Fig. 12). The high values of binding energies show the stiffness of the interaction of inhibitors on the studied surface. It is found that carvacrol is the most effective inhibitor due to its benzoyl ring and functional groups. The delocalized electron systems of corrosion inhibitors are attributed to enhance the inhibition efficiency. The flat adsorption positions of α -terpinene, (E)- β -ocimene,

thymol and carvacrol inhibitors are most favorable on the studied surface.

3.4.3 MD Simulation

The adsorption processes of corrosion inhibitors (α -terpinene, (E)- β -ocimene, thymol and carvacrol) on Fe(110) surface in dynamic condition were investigated by MD simulations. On the other hand, the adsorption positions of inhibitors on the metal surface were also studied in dynamic conditions. The most energetic stable positions of inhibitors are found by studying the temperature variations in MD

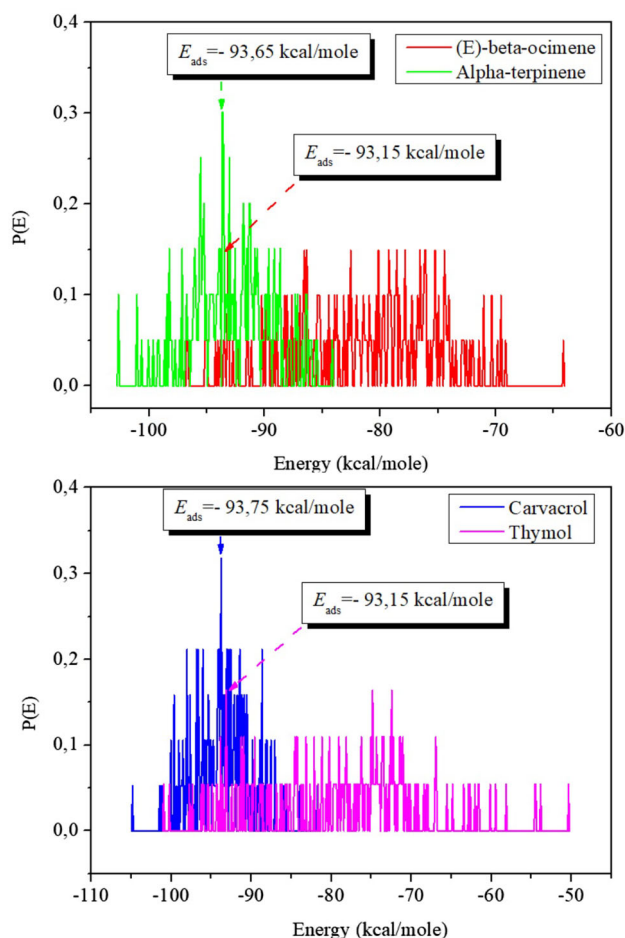


Fig. 12 Values of E_{ads} for α -terpinene, (E)- β -ocimene, thymol and carvacrol onto the Fe(110) surface

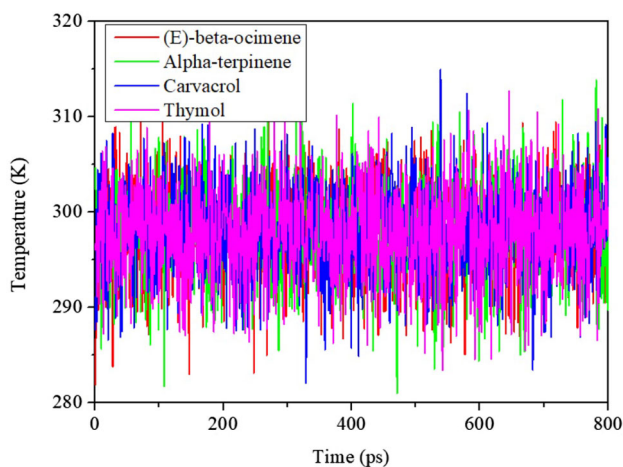


Fig. 13 Changes in temperature of selected MD simulation system (α -terpinene, (E)- β -ocimene, thymol and carvacrol, $T = 298$ K)

simulation analyses. As can be seen in Fig. 13, the temperature change is minimal, suggesting that the MD of the selected system was stable and effective [79, 85].

In the next part of the simulation analysis, the adsorption dynamics of α -terpinene, (E)- β -ocimene, thymol and carvacrol corrosion inhibitors on Fe (110) surface were investigated by the MD method and the obtained results are indicated in Fig. 14. In the corrosion inhibition analysis, the MD simulations were mostly used to describe the interaction between the optimized structures and metal surfaces [21, 23, 43, 44]. As observed, the α -terpinene, (E)- β -ocimene, thymol and carvacrol corrosion inhibitors adsorbed on Fe (110) surface by the flat adsorption positions. The water molecules and chloride atoms were insulated from the metal surface.

In the radial distribution (RDF) analysis, the bond distance between the adsorption centers and Fe atoms was estimated [86–88]. The obtained RDF plots are cited in Fig. 15. As can be seen from the obtained results, the distance between the oxygen heteroatom and Fe atom was under 3.5 \AA , confirming that the inhibitors adsorbed on the metal surface by the dominant chemisorption mechanism [3, 24]. The negative value of interaction energy shows that the α -terpinene, (E)- β -ocimene, thymol and carvacrol molecules are forcefully binding to the metal surface.

3.5 Adsorption Mechanism

The obtained results of electrochemical, surface and quantum chemical calculation methods suggested that the selected corrosion inhibitors adsorbed on the metal surface by the chemisorption and physisorption mechanisms. In addition to this, the given theoretical investigations demonstrate a strong agreement with electrochemical experiments, which demonstrate that these inhibitors have a great performance against metal corrosion [20, 89].

As indicated in Fig. 16, the lone pair electrons of the $-\text{OH}$ group, the π -electrons of the benzene ring and the double bonds may share their electrons with the empty D-orbitals of the Fe atoms, resulting in the chemisorption [78]. Next, the accumulated electrons of the D-orbitals of metal atoms lead to inter-electron repulsions. As a result, some electrons are transferred to the antibonding orbitals of benzoyl rings. These processes promote the formation of protective film.

The comparison results with the previously published works are tabulated in Table 9. It is indicated that the suggested *Oregano* extract is more effective at low concentrations. It was extracted with easy operation and cost-effective methods. The corrosion efficiency of *Oregano* extract is more stable at high temperatures.

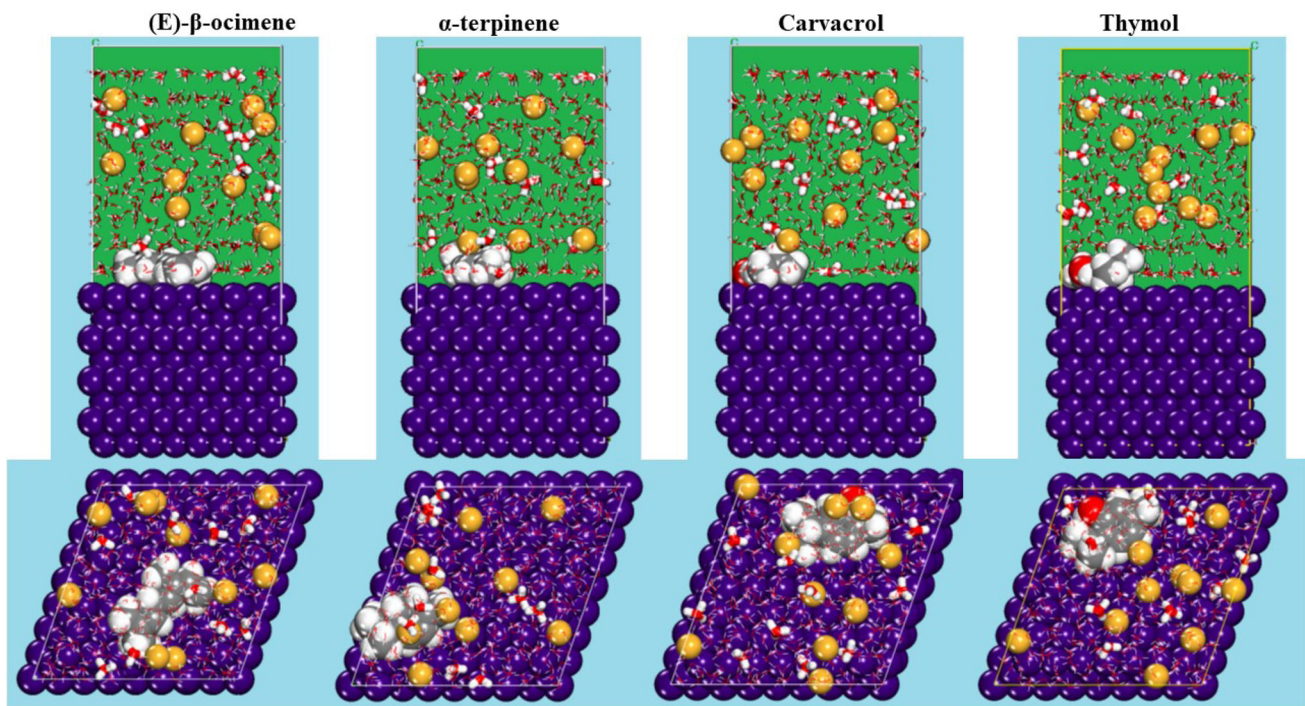


Fig. 14 Adsorption configurations and positions of α -terpinene, (E)- β -ocimene, thymol and carvacrol inhibitors on the Fe(110) surface

4 Conclusion

- In this research work, the following conclusions are found:
- Oregano extract is a more effective inhibitor for steel corrosion in aggressive acidic solutions at low concentrations. It was extracted with easy operation and cost-effective methods.
- Its maximum protection ability was 85.64% at 2 g/l at medium temperatures.
- The PDP method revealed that the introduction of this extract to a corrosive solution leads to a noticeable decrease in the i_{CORR} and both cathodic and anodic slopes of carbon steel.
- The polarizing activities on the cathodic and anodic regions were maximally blocked by the presence of this extract.
- Calculated thermodynamic parameters prove that this inhibitor acts by physical-sorption and chemical sorption mechanisms at the metal/electrolyte interface.
- MD calculations indicated that inhibitors flat-adsorbed onto the metal surface and their adsorption energies are fairly high.

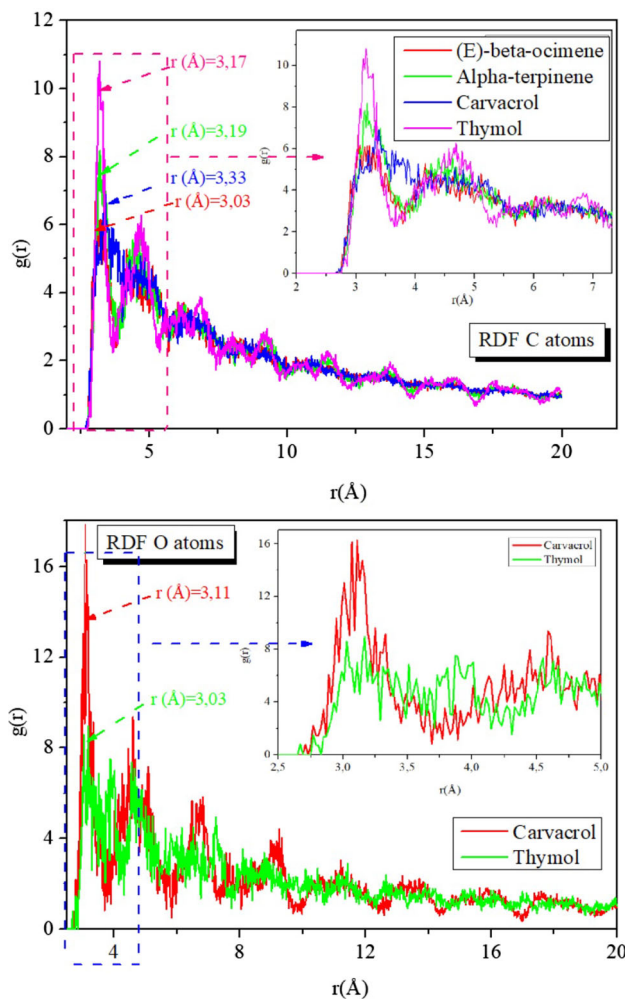


Fig. 15 RDF curves of α -terpinene, (E)- β -ocimene, thymol and carvacrol molecules

Fig. 16 A pictorial illustration of Carvacrol corrosion inhibitor on the steel surface

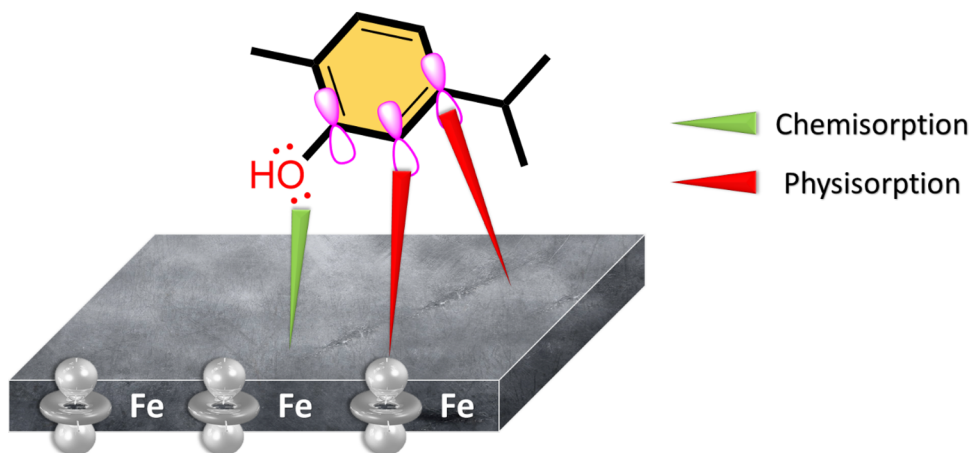


Table 9 Comparison results with the previous works (2 g/l, 1 M HCl, Steel)

Inhibitor	Method	IE (%)	Refs.
Citrus peel	WL	90	[90]
Spirogyra algae	EIS	67	[91]
Glycine max	EIS	86	[91]
Cuscuta reflexa	EIS	80	[91]
Cedrus atlantica	EIS	80	[92]
Watermelon rind	EIS	83	[93]
Watermelon seed	EIS	85	[93]
Watermelon peel	EIS	79	[93]
Phoenix dactylifera	EIS	88	[94]
Ircinia strobilina crude	WL	82	[95]
Origanum vulgare	EIS	87	Present work

Acknowledgements OD thankfully acknowledges the Centre for Materials Science, College of Science, Engineering and Technology, University of South Africa, for providing financial assistance under the postdoctoral fellowship scheme. AB expresses gratitude to the Kosovo Ministry of Education, Science, and Technology (Nr.2-5069) for their assistance in providing computing resources.

Author Contributions All the authors contributed equally to the manuscript.

Funding Open access funding provided by University of South Africa.

Declarations

Conflicts of interest Authors confirm that they have no conflict of interest.

Open Access This article is licensed under a Creative Commons Attribution 4.0 International License, which permits use, sharing, adaptation, distribution and reproduction in any medium or format, as long as you give appropriate credit to the original author(s) and the source, provide a link to the Creative Commons licence, and indicate if changes were made. The images or other third party material in this article are included in the article's Creative Commons licence, unless indicated otherwise in a credit line to the material. If material is not included in the article's Creative Commons licence and your intended use is not permitted by statutory regulation or exceeds the permitted use, you will need to obtain permission directly from the copyright holder. To view a copy of this licence, visit <http://creativecommons.org/licenses/by/4.0/>.

References

- Li, M., et al.: Inhibition performances of imidazole derivatives with increasing fluorine atom contents in anions against carbon steel corrosion in 1 M HCl. *J. Mol. Liq.* **322**, 114535 (2021)
- Dagdag, O., et al.: Recent progress in epoxy resins as corrosion inhibitors: design and performance. *J. Adhes. Sci. Technol.* **21**, 1–22 (2022)
- Dagdag, O., et al.: Designing of phosphorous based highly functional dendrimeric macromolecular resin as an effective coating material for carbon steel in NaCl: computational and experimental studies. *J. Appl. Polym. Sci.* **138**(2), 49673 (2021)
- Thirumoolan, D., et al.: Corrosion resistant performance of hydrophobic poly(N-vinyl imidazole-co-ethyl methacrylate) coating on mild steel. *Prog. Org. Coat.* **89**, 181–191 (2015)
- Dagdag, O., et al.: Epoxy prepolymer as a novel anti-corrosive material for carbon steel in acidic solution: electrochemical, surface and computational studies. *Mater. Today Commun.* **22**, 100800 (2020)
- Hsissou, R., et al.: Trifunctional epoxy polymer as corrosion inhibition material for carbon steel in 1.0 M HCl: MD simulations, DFT and complexation computations. *Inorg. Chem. Commun.* **115**, 107858–107858 (2020)
- Dagdag, O., et al.: Anticorrosive property of heterocyclic based epoxy resins on carbon steel corrosion in acidic medium: electrochemical, surface morphology, DFT and Monte Carlo simulation studies. *J. Mol. Liq.* **287**, 110977 (2019)
- Keleş, H.; Keleş, M.; Sayın, K.: Experimental and theoretical investigation of inhibition behavior of 2-((4-(dimethylamino) benzylidene) amino) benzenethiol for carbon steel in HCl solution. *Corros. Sci.* **184**, 109376 (2021)
- Berdimurodov, E., et al.: Inhibition properties of 4, 5-dihydroxy-4, 5-di-p-tolylimidazolidine-2-thione for use on carbon steel in an aggressive alkaline medium with chloride ions: thermodynamic, electrochemical, surface and theoretical analyses. *J. Mol. Liq.* **327**, 114813 (2021)
- Berdimurodov, E., et al.: New anti-corrosion inhibitor (3ar, 6ar)-3a, 6a-di-p-tolyltetrahydroimidazo [4, 5-d] imidazole-2, 5 (1 h, 3h)-dithione for carbon steel in 1 M HCl medium: gravimetric, electrochemical, surface and quantum chemical analyses. *Arab. J. Chem.* **13**(10), 7504–7523 (2020)
- Shaban, S.M., et al.: Corrosion inhibition and surface examination of carbon steel 1018 via N-(2-(2-hydroxyethoxy) ethyl)-N, N-dimethyloctan-1-aminiun bromide in 1.0 M HCl. *J. Mol. Struct.* **1227**, 129713 (2021)
- Damej, M., et al.: The corrosion inhibition and adsorption behavior of mercaptobenzimidazole and bis-mercaptobenzimidazole on carbon steel in 1.0 M HCl: experimental and computational insights. *Surf. Interfaces* **24**, 101095 (2021)
- Quadri, T.W., et al.: Computational insights into quinoxaline-based corrosion inhibitors of steel in HCl: quantum chemical analysis and QSPR-ANN studies. *Arab. J. Chem.* **15**(7), 103870 (2022)
- Chkirate, K., et al.: Corrosion inhibition potential of 2-[(5-methylpyrazol-3-yl) methyl] benzimidazole against carbon steel corrosion in 1 M HCl solution: combining experimental and theoretical studies. *J. Mol. Liq.* **321**, 114750 (2021)
- Haldhar, R., et al.: Corrosion inhibition, surface adsorption and computational studies of *Swertia chirata* extract: a sustainable and green approach. *Mater. Chem. Phys.* **267**, 124613 (2021)
- Berdimurodov, E., et al.: New and green corrosion inhibitor based on new imidazole derivate for carbon steel in 1 M Hcl medium: experimental and theoretical analyses. *Int. J. Eng. Res. Africa* **58**, 11 (2022)
- Dehghani, A., et al.: Potential role of a novel green eco-friendly inhibitor in corrosion inhibition of mild steel in HCl solution: detailed macro/micro-scale experimental and computational explorations. *Constr. Build. Mater.* **245**, 118464 (2020)
- Haldhar, R., et al.: Evaluation of *Gloriosa superba* seeds extract as corrosion inhibition for low carbon steel in sulfuric acidic medium: a combined experimental and computational studies. *J. Mol. Liq.* **323**, 114958 (2021)
- Rostami-Vartooni, A., et al.: Photocatalytic degradation of azo dyes by titanium dioxide supported silver nanoparticles prepared by a green method using *Carpobrotus acinaciformis* extract. *J. Alloy. Compd.* **689**, 15–20 (2016)
- Bhardwaj, N., et al.: Monte Carlo simulation, molecular dynamic simulation, quantum chemical calculation and anti-corrosive behaviour of Citrus limetta pulp waste extract for stainless steel (SS-410) in acidic medium. *Mater. Chem. Phys.* **284**, 126052 (2022)
- Haldhar, R., et al.: Anticorrosive properties of a green and sustainable inhibitor from leaves extract of *Cannabis sativa* plant: experimental and theoretical approach. *Colloids Surf., A* **614**, 126211 (2021)
- Dewangan, Y., et al.: N-hydroxypyrazine-2-carboxamide as a new and green corrosion inhibitor for mild steel in acidic medium: experimental, surface morphological and theoretical approach. *J. Adhes. Sci. Technol.* **12**, 1–21 (2022)
- Berdimurodov, E., et al.: Novel glycoluril pharmaceutically active compound as a green corrosion inhibitor for the oil and gas industry. *J. Electroanal. Chem.* **524**, 116055 (2022)
- Berdimurodov, E., et al.: Novel gossypol–indole modification as a green corrosion inhibitor for low–carbon steel in aggressive alkaline–saline solution. *Colloids Surf. A Physicochem. Eng. Aspects* **235**, 128207 (2022)
- Shahmoradi, A., et al.: Theoretical and surface/electrochemical investigations of walnut fruit green husk extract as effective inhibitor for mild-steel corrosion in 1M HCl electrolyte. *J. Mol. Liq.* **338**, 116550 (2021)
- Berdimurodov, E., et al.: Novel cucurbit [6] uril-based [3] rotaxane supramolecular ionic liquid as a green and excellent corrosion inhibitor for the chemical industry. *Colloids Surf., A* **633**, 127837 (2022)
- Berdimurodov, E., et al.: Novel bromide–cucurbit [7] uril supramolecular ionic liquid as a green corrosion inhibitor for the oil and gas industry. *J. Electroanal. Chem.* **901**, 115794 (2021)
- Berdimurodov, E., et al.: Experimental and theoretical assessment of new and eco–friendly thioglycoluril derivative as an effective corrosion inhibitor of St2 steel in the aggressive hydrochloric acid with sulfate ions. *J. Mol. Liq.* **335**, 116168 (2021)
- Verma, D.K., et al.: N–hydroxybenzothioamide derivatives as green and efficient corrosion inhibitors for mild steel: experimental, DFT and MC simulation approach. *J. Mol. Struct.* **1241**, 130648 (2021)



30. de Souza, F.S., et al.: Adsorption behavior of caffeine as a green corrosion inhibitor for copper. *Mater. Sci. Eng. C* **32**(8), 2436–2444 (2012)
31. Zhu, M., et al.: Insights into the newly synthesized N-doped carbon dots for Q235 steel corrosion retardation in acidizing media: a detailed multidimensional study. *J. Colloid Interface Sci.* **608**, 2039–2049 (2022)
32. Haldhar, R., et al.: Corrosion inhibition, surface adsorption and computational studies of *Momordica charantia* extract: a sustainable and green approach. *SN Appl. Sci.* **3**(1), 1–13 (2021)
33. Benabida, A., et al.: Potentials of nigella sativa oil as inhibition towards the corrosion of mild steel in neutral media. (2016)
34. Figiel, A., et al.: Composition of oregano essential oil (*Origanum vulgare*) as affected by drying method. *J. Food Eng.* **98**(2), 240–247 (2010)
35. Ghanmi, M., et al.: Essential oils from *Origanum compactum* as an alternative active ingredient against wood decay fungi. (2015)
36. Yukna, R.A., et al.: Multi-center clinical evaluation of combination anorganic bovine-derived hydroxyapatite matrix (ABM)/cell binding peptide (P-15) as a bone replacement graft material in human periodontal osseous defects 6-month results. *J. Periodontol.* **69**(6), 655–663 (1998)
37. Andzelm, J.; King-Smith, R.; Fitzgerald, G.: Geometry optimization of solids using delocalized internal coordinates. *Chem. Phys. Lett.* **335**(3–4), 321–326 (2001)
38. Inada, Y.; Orita, H.: Efficiency of numerical basis sets for predicting the binding energies of hydrogen bonded complexes: evidence of small basis set superposition error compared to Gaussian basis sets. *J. Comput. Chem.* **29**(2), 225–232 (2008)
39. Sun, J.; Ruzsinszky, A.; Perdew, J.P.: Strongly constrained and appropriately normed semilocal density functional. *Phys. Rev. Lett.* **115**(3), 036402 (2015)
40. Dasgupta, S., et al.: Elevating density functional theory to chemical accuracy for water simulations through a density-corrected many-body formalism. *Nat. Commun.* **12**(1), 1–12 (2021)
41. Berisha, A.: Interactions between the aryl diazonium cations and graphene oxide: a DFT study. *J. Chem.* **2019**, 703 (2019)
42. Alija, A., et al.: A theoretical and experimental study of the adsorptive removal of hexavalent chromium ions using graphene oxide as an adsorbent. *Open Chem.* **18**(1), 936–942 (2020)
43. Berisha, A.: Experimental, Monte Carlo and molecular dynamic study on corrosion inhibition of mild steel by pyridine derivatives in aqueous perchloric acid. *Electrochem* **1**(2), 188–199 (2020)
44. Hsissou, R., et al.: Evaluation of corrosion inhibition performance of phosphorus polymer for carbon steel in [1 M] HCl: computational studies (DFT, MC and MD simulations). *J. Market. Res.* **9**(3), 2691–2703 (2020)
45. Rbaa, M., et al.: Simple preparation and characterization of novel 8-Hydroxyquinoline derivatives as effective acid corrosion inhibitor for mild steel: experimental and theoretical studies. *Colloids Surf. A* **602**, 125094 (2020)
46. Hsissou, R., et al.: Novel derivative epoxy resin TGETET as a corrosion inhibition of E24 carbon steel in 1.0 M HCl solution: experimental and computational (DFT and MD simulations) methods. *J. Mol. Liq.* **284**, 182–192 (2019)
47. Dagdag, O., et al.: DGEBA-polyaminoamide as effective anti-corrosive material for 15CDV6 steel in NaCl medium: computational and experimental studies. *J. Appl. Polym. Sci.* **137**(8), 48402 (2020)
48. Dagdag, O., et al.: Fabrication of polymer based epoxy resin as effective anti-corrosive coating for steel: computational modeling reinforced experimental studies. *Surf. Interfaces* **18**, 100454 (2020)
49. Dagdag, O., et al.: Polymeric-based epoxy cured with a polyaminoamide as an anticorrosive coating for aluminum 2024–T3 surface: experimental studies supported by computational modeling. *J. Bio-Tribo-Corr.* **5**(3), 1–13 (2019)
50. El Faydy, M., et al.: An experimental-coupled empirical investigation on the corrosion inhibitory action of 7-alkyl-8-Hydroxyquinolines on C35E steel in HCl electrolyte. *J. Mol. Liq.* **317**, 113973 (2020)
51. Dagdag, O., et al.: Epoxy resins and their zinc composites as novel anti-corrosive materials for copper in 3% sodium chloride solution: experimental and computational studies. *J. Mol. Liq.* **315**, 113757 (2020)
52. Dagdag, O., et al.: Epoxy coating as effective anti-corrosive polymeric material for aluminum alloys: formulation, electrochemical and computational approaches. *J. Mol. Liq.* **346**, 117886 (2022)
53. Mzioud, K., et al.: Inhibition of copper corrosion by the essential oil of *Allium sativum* in 0.5 M H₂SO₄ solutions. *SN Appl. Sci.* **2**(9), 1–13 (2020)
54. Liu, Y., et al.: Study on adsorption behavior of ketoconazole on Q235 mild steel in 1.0 M HCl solution with electrochemical measurement. *J. Alloys Comp.* **758**, 184–193 (2018)
55. Hegazy, M.; Atlam, F.: Three novel bolaamphiphiles as corrosion inhibitors for carbon steel in hydrochloric acid: experimental and computational studies. *J. Mol. Liq.* **218**, 649–662 (2016)
56. Chaouiki, A., et al.: Understanding corrosion inhibition of mild steel in acid medium by new benzonitriles: insights from experimental and computational studies. *J. Mol. Liq.* **266**, 603–616 (2018)
57. Qian, B., et al.: Synergistic effect of polyaspartic acid and iodide ion on corrosion inhibition of mild steel in H₂SO₄. *Corros. Sci.* **75**, 184–192 (2013)
58. Mourya, P., et al.: Inhibition of mild steel corrosion by 1, 4, 6-trimethyl-2-oxo-1, 2-dihydropyridine-3-carbonitrile and synergistic effect of halide ion in 0.5 M H₂SO₄. *Appl. Surf. Sci.* **380**, 141–150 (2016)
59. Dagdag, O., et al.: Epoxy pre-polymers as new and effective materials for corrosion inhibition of carbon steel in acidic medium: computational and experimental studies. *Sci. Rep.* **9**(1), 1–14 (2019)
60. Chevalier, M., et al.: Investigation of corrosion inhibition efficiency of Amazonian tree alkaloids extract for C38 steel in 1M hydrochloric media. *Int. J. Electrochem. Sci.* **215**, 1208–1223 (2019)
61. Ouici, H., et al.: Adsorption and corrosion inhibition properties of 5-amino 1, 3, 4-thiadiazole-2-thiol on the mild steel in hydrochloric acid medium: Thermodynamic, surface and electrochemical studies. *J. Electroanal. Chem.* **803**, 125–134 (2017)
62. Ouakki, M., et al.: Insights into corrosion inhibition mechanism of mild steel in 1 M HCl solution by quinoxaline derivatives: electrochemical, SEM/EDAX, UV-visible, FT-IR and theoretical approaches. *Colloids Surf. A* **611**, 125810 (2021)
63. Hossain, S.; Razzak, S.; Hossain, M.: Application of essential oils as green corrosion inhibitors. *Arab. J. Sci. Eng.* **45**(9), 7137–7159 (2020)
64. Dhoubi, I., et al.: A study of the anti-corrosive effects of essential oils of rosemary and myrtle for copper corrosion in chloride media. *Arab. J. Chem.* **14**(2), 102961 (2021)
65. Jmiai, A., et al.: Alginate biopolymer as green corrosion inhibitor for copper in 1 M hydrochloric acid: experimental and theoretical approaches. *J. Mol. Struct.* **1157**, 408–417 (2018)
66. Dkhireche, N., et al.: New quinoline derivatives as sulfuric acid inhibitor's for mild steel. *Anal. Bioanal. Electrochem.* **10**(1), 111–135 (2018)
67. Nabah, R., et al.: Corrosion inhibition study of 5, 5-diphenylimidazolidine-2, 4-dione for mild steel corrosion in 1 M HCl solution: experimental, theoretical computational and Monte Carlo simulations studies. 2018
68. Popova, A.: Temperature effect on mild steel corrosion in acid media in presence of azoles. *Corr. Sci.* **49**(5), 2144–2158 (2007)
69. Hongbo, F.: Synthesis and application of new type inhibitors. Chemical Industry Press, Beijing (2002)



70. Rbaa, M., et al.: Adsorption properties and inhibition of carbon steel corrosion in a hydrochloric solution by 2-(4, 5-diphenyl-4, 5-dihydro-1h-imidazol-2-yl)-5-methoxyphenol. *Electrochim. Acta* **35**(6), 323–338 (2017)
71. Boughoues, Y., et al.: Adsorption and corrosion inhibition performance of some environmental friendly organic inhibitors for mild steel in HCl solution via experimental and theoretical study. *Colloids Surf. A* **593**, 124610 (2020)
72. Damej, M., et al.: New epoxy resin as a corrosion inhibitor for the protection of carbon steel C38 in 1M HCl experimental and theoretical studies (DFT, MC, and MD). *J.Mol. Struct.* **124**, 132425 (2022)
73. Bhardwaj, N., et al.: Monte Carlo simulation, molecular dynamic simulation, quantum chemical calculation and anti-corrosive behaviour of Citrus limetta pulp waste extract for stainless steel (SS-410) in acidic medium. *Mater. Chem. Phys.* **284**, 126052 (2022)
74. Jafari, H., et al.: Anti-corrosion behavior of two N2O4 Schiff-base ligands: Experimental and theoretical studies. *J. Phys. Chem. Solids* **164**, 110645 (2022)
75. Abdelwedoud, B.O., et al.: Inhibition effect of N-propargyl saccharin as corrosion inhibitor of C38 steel in 1 M HCl, experimental and theoretical study. *J. Mol. Liq.* **354**, 118784 (2022)
76. Berisha, A.; Podvorica, F.I.; Vataj, R.: Corrosion inhibition study of mild steel in an aqueous hydrochloric acid solution using brilliant cresyl blue—a combined experimental and monte carlo study. *Electrochim. Acta* **39**, 393–401 (2021)
77. Mehmeti, V.: Nystatin drug as an effective corrosion inhibitor for mild steel in acidic media-an experimental and theoretical study. *Corr. Sci. Technol.* **21**(1), 21–31 (2022)
78. Oukhrib, R., et al.: DFT, Monte Carlo and molecular dynamics simulations for the prediction of corrosion inhibition efficiency of novel pyrazolynucleosides on Cu (111) surface in acidic media. *Sci. Rep.* **11**(1), 1–18 (2021)
79. El Faydy, M., et al.: Insight into the corrosion inhibition of new bis-quinolin-8-ols derivatives as highly efficient inhibitors for C35E steel in 05 M H2SO4. *J. Mol. Liq.* **342**, 117333 (2021)
80. Berisha, A.: Ab initio exploration of nanocars as potential corrosion inhibitors. *Comput. Theor. Chem.* **1201**, 113258 (2021)
81. Berisha, A.: An Experimental and theoretical investigation of the efficacy of pantoprazole as a corrosion inhibitor for mild steel in an acidic medium. *Electrochim. Acta* **3**(1), 28–41 (2022)
82. Abdellatif, M.H., et al.: Calotropis procera extract as an environmental friendly corrosion inhibitor: computational demonstrations. *J. Mol. Liq.* **337**, 116954 (2021)
83. Haldhar, R., et al.: Papaver somniferum as an efficient corrosion inhibitor for iron alloy in acidic condition: DFT, MC simulation, LCMS and electrochemical studies. *J. Mol. Struct.* **542**, 130822 (2021)
84. Khalaf, B., et al.: Cellulose-based hectocycle nanopolymers: synthesis, molecular docking and adsorption of difenoconazole from aqueous medium. *Int. J. Mol. Sci.* **22**(11), 6090 (2021)
85. Molhi, A., et al.: Performance of two epoxy resins against corrosion of C38 steel in 1M HCl: electrochemical, thermodynamic and theoretical assessment. *Int. J. Corr. Scale Inhib* **10**(2), 812–837 (2021)
86. Bhardwaj, N., et al.: Molecular dynamic simulation and Quantum chemical calculation of phytochemicals present in Beta vulgaris and electrochemical behaviour of Beta vulgaris peel extract as green corrosion inhibitor for stainless steel (SS-410) in acidic medium. *Colloids Surf. A* **632**, 127707 (2022)
87. Dagdag, O., et al.: Development and anti-corrosion performance of polymeric epoxy resin and their zinc phosphate composite on 15CDV6 steel in 3wt% NaCl: experimental and computational studies. *J. Bio- Tribo-Corr.* **6**(4), 1–9 (2020)
88. Dagdag, O., et al.: Cyclotriphosphazene based dendrimeric epoxy resin as an anti-corrosive material for copper in 3% NaCl: experimental and computational demonstrations. *J. Mol. Liq.* **308**, 113020 (2020)
89. Rahimi, A., et al.: Novel sucrose derivative as a thermally stable inhibitor for mild steel corrosion in 15% HCl medium: an experimental and computational study. *Chem. Eng. J.* **245**, 136938 (2022)
90. Fiori-Bimbi, M.V., et al.: Corrosion inhibition of mild steel in HCL solution by pectin. *Corr. Sci.* **92**, 192–199 (2015)
91. Verma, D., et al.: Inhibition performance of Glycine max, Cuscuta reflexa and Spirogyra extracts for mild steel dissolution in acidic medium: density functional theory and experimental studies. *Results Phys.* **10**, 665–674 (2018)
92. Idouhli, R., et al.: Inhibitory effect of Senecio anteuphorbium as green corrosion inhibitor for S300 steel. *Int. J. Ind. Chem.* **10**(2), 133–143 (2019)
93. Odewunmi, N.; Umoren, S.; Gasem, Z.: Watermelon waste products as green corrosion inhibitors for mild steel in HCl solution. *J. Environ. Chem. Eng.* **3**(1), 286–296 (2015)
94. Umoren, S.; Gasem, Z.; Obot, I.: Date palm (Phoenix dactylifera) leaf extract as an eco-friendly corrosion inhibitor for carbon steel in 1M hydrochloric acid solution. *Anti-Corr. Methods Mater.* **12**, 563 (2015)
95. Fernandes, C.M., et al.: Ircinia strobilina crude extract as corrosion inhibitor for mild steel in acid medium. *Electrochim. Acta* **312**, 137–148 (2019)

